



**HAL**  
open science

## Synthesis of iron-rich tri-octahedral clay minerals: A review

Liva Dzene, Jocelyne Brendle, Lionel Limousy, Patrick Dutournie, Christelle Martin, Nicolas Michau

### ► To cite this version:

Liva Dzene, Jocelyne Brendle, Lionel Limousy, Patrick Dutournie, Christelle Martin, et al.. Synthesis of iron-rich tri-octahedral clay minerals: A review. *Applied Clay Science*, 2018, 166, pp.276-287. 10.1016/j.clay.2018.09.030 . hal-02288179

**HAL Id: hal-02288179**

**<https://hal.science/hal-02288179v1>**

Submitted on 13 Sep 2019

**HAL** is a multi-disciplinary open access archive for the deposit and dissemination of scientific research documents, whether they are published or not. The documents may come from teaching and research institutions in France or abroad, or from public or private research centers.

L'archive ouverte pluridisciplinaire **HAL**, est destinée au dépôt et à la diffusion de documents scientifiques de niveau recherche, publiés ou non, émanant des établissements d'enseignement et de recherche français ou étrangers, des laboratoires publics ou privés.

# Synthesis of iron-rich tri-octahedral clay minerals: A review

Liva Dzene<sup>1, \*</sup>, Jocelyne Brendle<sup>1</sup>, Lionel Limousy<sup>1</sup>, Patrick Dutournie<sup>1</sup>, Christelle Martin<sup>2</sup>  
and Nicolas Michau<sup>2</sup>

<sup>1</sup>Institut de Science des Matériaux de Mulhouse CNRS UMR 7361, Université de Haute-Alsace, Université de Strasbourg, 3b rue Alfred Werner, 68093 Mulhouse CEDEX, France

<sup>2</sup>Andra, R&D Division, Materials & Waste packages Department, 1/7 rue Jean Monnet, F-92298 Châtenay-Malabry CEDEX, France

\*liva.dzene@uha.fr

## Abstract

Examples in materials science and in geology show an interest for iron-rich tri-octahedral clay mineral synthesis in large amounts and with well-defined characteristics. This review summarizes previously reported methods and conditions for iron-rich tri-octahedral clay mineral synthesis. Two approaches of hydrothermal synthesis have been applied: using gel or solid precursors. The most common synthesis approach is the hydrothermal synthesis using gel precursor. The synthesis of 1:1 type clay minerals were performed in reducing conditions in neutral or alkaline pH at various temperature and time ranges. The experimental conditions for 2:1 type clay mineral synthesis were in most cases similar to 1:1 type clay minerals, with in addition acidic pH and oxidizing conditions. The most commonly used methods for identifying and characterizing these minerals are X-ray diffraction, infra-red and Mössbauer spectroscopies as well as transmission electron microscopy. The thermodynamic stability of synthesized phases, as well as the reason for elements adopting a definite configuration and distribution in solid phase remain open questions.

**Keywords** : greenalite, cronstedtite, hydrothermal synthesis, iron-rich clay minerals, serpentine

## 24 **1. Introduction**

25 Iron-rich tri-octahedral clay minerals have a high potential as heterogeneous catalyst,  
26 e.g. in Fenton-like reactions (Garrido-Ramírez et al., 2010; Li et al., 2015; Wang et al., 2017)  
27 and some organic transformations (Arundhathi et al., 2011, 2010; Sreedhar et al., 2009). In  
28 nature, these minerals are found in ocean floors, where the serpentinization of olivines occurs  
29 (Kodolányi et al., 2012), but such formations are either not easily accessible or not largely  
30 abundant. Moreover, natural minerals often contain other mineral phases, which can be  
31 considered as impurities for certain applications. To obtain a sufficient amount of pure iron-  
32 rich tri-octahedral clay minerals and to study their potential application in catalysis, their  
33 synthesis can be foreseen.

34 Apart for the interest of the application in materials science, clay minerals are also  
35 present in deep-geological formations envisaged for CO<sub>2</sub> sequestration or nuclear waste  
36 disposal (Bourg, 2015; Grambow, 2016). To predict a long-term stability of these formations,  
37 geochemical modelling is often performed, but the lack of thermodynamic data regarding iron-  
38 rich tri-octahedral clay minerals places limits to these models. An investigation of the  
39 thermodynamic properties of synthetic iron-rich tri-octahedral clay minerals as analogues to  
40 naturally formed minerals could provide the missing data. Thus, this could improve our  
41 understanding of the long-term stability of these minerals and the respective geological  
42 formations in which their natural analogues are present.

43 The third aspect, where the importance of the presence of iron-rich swelling clay  
44 minerals has been suggested is the formation of the first biopolymers on Earth surface (Feuillie  
45 et al., 2013; Meunier et al., 2010; Pedreira-Segade et al., 2016). A series of synthetic iron-rich  
46 tri-octahedral clay minerals with well-defined characteristics, such as particle size and layer  
47 charge could contribute to understanding the adsorption and retention phenomena of these  
48 molecules on clay surfaces.

49 Finally, the presence of iron-rich tri-octahedral clay minerals has been observed on the  
50 surface of Mars (Chemtob et al., 2015), in deep-sea sediments (Baldermann et al., 2015; Tosca  
51 et al., 2016), during the chloritization (Beaufort et al., 2015) and serpentinization (Kodolányi  
52 et al., 2012) in subduction zones and transform faulting, in meteorites (Zolotov, 2015), but the  
53 formation conditions remain poorly understood. Their synthesis under well-controlled  
54 conditions and parameters could help to understand these phenomena. Previously mentioned  
55 examples in materials science and in geology show an interest for iron-rich tri-octahedral clay  
56 mineral synthesis in sufficient quantities and with well-defined characteristics. The first report  
57 of iron-rich tri-octahedral clay mineral synthesis dates back to 1911 (Van Hise and Leith, 1911),  
58 but there has been a growing interest particularly in the latest years (Baldermann et al., 2014;  
59 Chemtob et al., 2015; Tosca et al., 2016). Although three general reviews on clay mineral  
60 synthesis by Kloprogge et al. (1999), Zhang et al. (2010) and Jaber et al. (2013) exist, as well  
61 as a review of Petit et al. (2017) on Fe-rich smectites has been recently published, ferrous iron-  
62 rich systems are very particular in terms of synthesis conditions (atmosphere, redox potential)  
63 and characterization, making it necessary for a separate review. Three different clay mineral  
64 synthesis techniques are known : synthesis from dilute solution, solid-state and hydrothermal  
65 synthesis (Carrado et al., 2006). Different variations of hydrothermal synthesis technique have  
66 been used to form iron-rich tri-octahedral clay minerals (IRTOCM). They can be divided into  
67 two groups based on the type of precursor used: (1) hydrothermal synthesis using gel precursor  
68 and (2) hydrothermal synthesis using solid precursor. These two groups are discussed in this  
69 review focusing on the initial reactants, conditions, and procedures. This information is then  
70 summarized with respect to each mineral type: saponite (2:1 type), serpentine (1:1 type) and  
71 chlorite groups. The spectroscopic methods used to characterize iron-rich clay minerals have  
72 been previously summarized (Neumann et al., 2011), therefore only brief description of  
73 techniques used for IRTOCM identification is mentioned. At the end, the use of IRTOCM in

74 geochemical simulations and the influence of element speciation in solution on the neoformed  
75 phases are discussed.

## 76 **2. Hydrothermal synthesis based on the use of gel precursor**

### 77 *2.1. Procedure of synthesis*

78 The hydrothermal synthesis method based on the use of gel precursor is the most  
79 common to form IRTOCM. A general procedure composed of five steps can be suggested  
80 (Figure 1):

- 81 1) preparation of a precursor;
- 82 2) gel processing;
- 83 3) hydrothermal treatment;
- 84 4) product processing;
- 85 5) storage.

#### 86 *2.1.1. Preparation of a precursor*

87 The synthesis procedure starts with the preparation of a precursor, where an exact  
88 known mass of solid compounds or a defined volume of solutions is taken in stoichiometric  
89 proportions corresponding to the desired chemical composition of the product. In both cases,  
90 whether solid compounds or solutions are used, there are two ways of combining the  
91 constituents. In the first case, the order of mixing is the following: (1) metal Fe, Mg or Al salt  
92 solutions, (2) source of Si and (3) mineralizing agent (e.g., OH<sup>-</sup>). In the second case, the salt  
93 solution containing Fe, Mg and/or Al (A) and a solution containing Si and OH<sup>-</sup> (B) are mixed  
94 separately. Then solution (B) is slowly added to solution (A). After the addition of all the  
95 compounds, precipitation of solid phase occurs, often as a gel. A gel is a non-fluid colloidal  
96 network containing lamellar or disordered structures that are expanded throughout whole

97 volume of gel by a fluid (McNaught and Wilkinson, 1997). Less often, precipitated solid phase  
98 remains dispersed in the solution in form of suspension. Ideally, the preparation of precursor  
99 should result in a homogenous distribution of various elements in the gel matrix (Hamilton and  
100 Henderson, 1968), but in practice the formation of clusters of elements can occur. This can  
101 generate a heterogeneous distribution of certain elements in the precursor and subsequently the  
102 final product can also exhibit some sort of heterogeneity. After the preparation of precursor,  
103 depending of the metal source, washing or heating of precipitate can be performed.

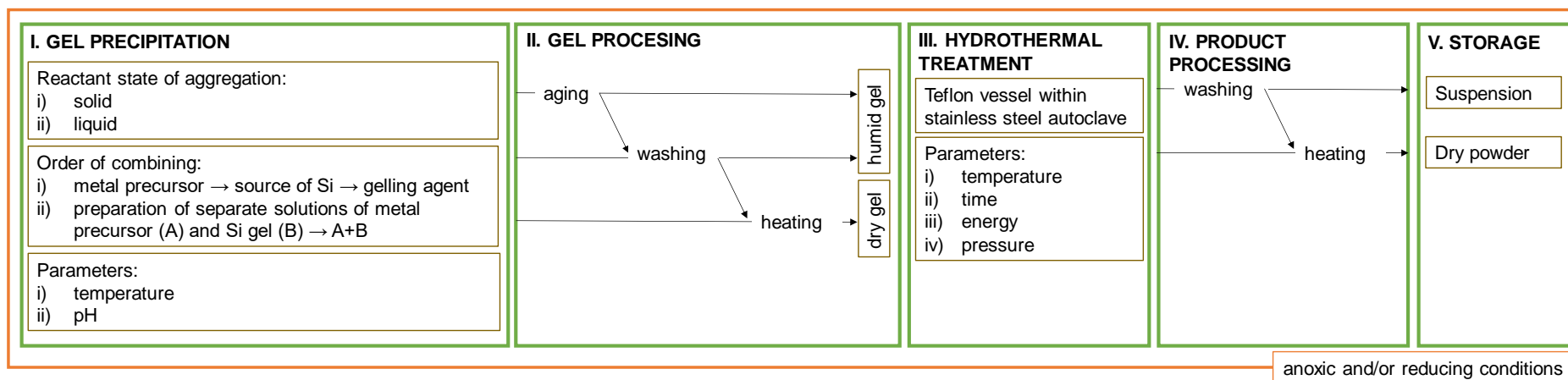
#### 104 *2.1.2. Different types of subsequent precursor treatment*

105 Three different approaches can be distinguished for the following synthesis procedure.  
106 The first type of approach consists of a gel aging step only. After precipitation of the solid  
107 phase, the dispersion is left to age for several weeks or months (Decarreau, 1981; Farmer et al.,  
108 1991; Harder, 1978; Tosca et al., 2016). The gel aging step is performed at temperatures ranging  
109 from 3 °C to 120 °C. For the second approach, gel aging is followed by hydrothermal treatment  
110 (Chemtob et al., 2015; Grauby et al., 1994; Lantenois et al., 2005; Mizutani et al., 1991; Wilkins  
111 and Ito, 1967). The hydrothermal treatment step is performed in autoclaves at temperatures  
112 from 60 °C to 600 °C over the course of 1 day to 3 months. In the third approach, only  
113 hydrothermal treatment is applied (Baldermann et al., 2014; Boukili et al., 2015; Flaschen and  
114 Osborn, 1957; Grubb, 1971; Roy and Roy, 1954). Another approach, which was used to obtain  
115 the first synthetic clay minerals in laboratory but is no longer in use, consisted of precipitating  
116 the solid from dilute solutions at boiling temperature under reflux (Caillère et al., 1953).

117 A one-step synthesis consisting solely of a gel aging or hydrothermal step have been  
118 applied in the studies which focus on the formation conditions of IRTOCM in specific  
119 geological environments (Baldermann et al., 2014; Boukili et al., 2015; Chemtob et al., 2015;  
120 Decarreau, 1981; Farmer et al., 1991; Flaschen and Osborn, 1957; Grubb, 1971; Harder, 1978;  
121 Roy and Roy, 1954; Tosca et al., 2016; Van Hise and Leith, 1911). A two-step synthesis

122 including both gel-aging and hydrothermal steps has been applied in some cases, where a  
123 known and precise material chemical composition is needed (Grauby et al., 1994; Lantenois et  
124 al., 2005; Mizutani et al., 1991; Wilkins and Ito, 1967). The heating or washing of sample  
125 between the two steps allows removing salts such as nitrates and carbonates so that the  
126 precursor's chemical composition corresponds to the one expected for the final product. In  
127 practice, the complete washing of anions is impossible in a gel, therefore some deviation from  
128 'ideal composition' should be expected. A one-step procedure consisting solely of  
129 hydrothermal treatment could be applied in studies where simple and fast procedure is needed  
130 and the presence of impurities can be tolerated.

131



132

133 **Figure 1.** 5-block action scheme detailing the steps of hydrothermal synthesis procedure based on the use of gel precursor for iron-rich trioctahedral

134 clay minerals: (I) gel precipitation, (II) gel processing, (III) hydrothermal treatment, (IV) product processing and (V) sample storage.



### 135 2.1.3. *Product processing and storage*

136 The processing block includes washing and/or heating of the products. The washing  
137 procedure in order to remove the impurities within the neoformed products varies from one  
138 synthesis procedure to another, including steps such as centrifugation, filtration and dialysis.  
139 The purified synthesis products are then dried either under vacuum or by heating the samples  
140 at no more than 120 °C, or freeze-dried. The obtained product is stored as dry powder, except  
141 in one case (Baldermann et al., 2014), where it is kept as a dispersion in 6 % wt HNO<sub>3</sub> in order  
142 to limit the oxidation of Fe<sup>2+</sup>. The advantage of storing the solid as a dispersion is the possibility  
143 to easily dilute or dry a sample without altering its granulometry. Dispersion of clay minerals  
144 particles < 0.2 µm has been observed to be difficult, particularly after drying (Dzene, 2016).

## 145 2.2. *Synthesis reactants and conditions*

### 146 2.2.1. *Source of silicon*

147 For the synthesis of 1:1 and 2:1 clay minerals, the literature indicates that, tetraethyl  
148 orthosilicate (TEOS) Si(OC<sub>2</sub>H<sub>5</sub>)<sub>4</sub> (Boukili et al., 2015; Farmer et al., 1991; Flaschen and  
149 Osborn, 1957; Lantenois et al., 2005; Tosca et al., 2016) and sodium silicates (Na<sub>2x</sub>SiO<sub>2+x</sub>)  
150 (Baldermann et al., 2014; Chemtob et al., 2015; Decarreau, 1981; Grauby et al., 1994; Grubb,  
151 1971; Mizutani et al., 1991; Van Hise and Leith, 1911; Wilkins and Ito, 1967) have been  
152 identified as excellent sources of Si due to their high solubility in water. One convenience for  
153 the use of sodium silicates is the possibility to combine the addition of two elements, i.e., Na  
154 and Si, to the reaction mixture with the same reagent. It can be advantageous when looking for  
155 reducing total number of steps. However, if there is a necessity to use different Na/Si molar  
156 ratios other than can be obtained by sole use of sodium silicates, TEOS can be used as an  
157 alternative source. In such a way, it is possible to add an exact amount of Si and also an exact  
158 amount of Na with a different reagent. Ethanol, the by-product which forms after the TEOS  
159 hydrolysis, can be easily removed by washing or heating.

160 2.2.2. *Source of iron and other metals*

161 For the source of metals (Mg, Al, Fe) and the interlayer cations (e.g., Na<sup>+</sup>), the use of  
162 different salts such as sulfates, nitrates, chlorides and carbonates has been reported. The type  
163 of anion such as sulfates or chlorides has an effect on the subsequent synthesis procedure and  
164 on the obtained product (Miyawaki et al., 1991). Four groups of reaction by-products  
165 (impurities) which can potentially be formed in the reaction mixture can be distinguished:

- 166 1) soluble<sup>1</sup> and having low decomposition temperature <600 °C;
- 167 2) soluble and having high decomposition temperature >600 °C;
- 168 3) insoluble and having low decomposition temperature <600 °C;
- 169 4) insoluble and having high decomposition temperature >600 °C.

170 These by-products can be removed after precipitation of the gel by washing it with solvent or  
171 by heating or after the synthesis by washing with solvent. If soluble salts with low  
172 decomposition temperature (<600 °C) such as nitrates NO<sub>3</sub><sup>-</sup> are formed in reaction mixture,  
173 they can be removed at both stages. Soluble salts with high decomposition temperature  
174 (>600 °C) such as sulfates SO<sub>4</sub><sup>2-</sup> and Li<sub>2</sub>CO<sub>3</sub>, K<sub>2</sub>CO<sub>3</sub>, Na<sub>2</sub>CO<sub>3</sub> can be removed at both stages,  
175 but only by washing. The heating would not be a solution for such salts due to their high  
176 decomposition temperature. Insoluble salts with low decomposition temperature such as  
177 carbonates (except CaCO<sub>3</sub>, BaCO<sub>3</sub>, Li<sub>2</sub>CO<sub>3</sub>, K<sub>2</sub>CO<sub>3</sub>, Na<sub>2</sub>CO<sub>3</sub>) can be removed by heating after  
178 the precipitation of gel. Finally, the last group of impurities which can potentially form  
179 insoluble products with high decomposition temperature cannot be eliminated by washing or  
180 by heating, and thus should not be used in the synthesis. The summary of the impurity  
181 characteristics and the way of their removal from the reaction mixture is given in Table 1. Note

---

<sup>1</sup> Here and hereinafter, the solubility refers to solubility of >1 g/L in aqueous solutions at room conditions.

182 that the room conditions were considered for the given examples. Different parameters such as  
183 pH, temperature, pressure and solution composition can influence the compound solubility.

184 It has to be considered that during the gel precipitation, the reaction products may become  
185 entrained within a hydrogel matrix which contain reactive precursor gel and the impurities, so  
186 washing can result in loss of some reaction products as well as truncate formative reaction of  
187 products.

188         The influence of anions on the nature of the synthesis products has not been extensively  
189 investigated. Four experiments can be mentioned. Baron (2016) run an experiment comparing  
190 the use of FeCl<sub>2</sub> and FeSO<sub>4</sub> for the preparation of the precursor, which was later used in  
191 nontronite synthesis. FTIR spectra of precursors and their synthesis products were identical for  
192 both anions used. Thus, in this particular case, when the protocol involved the precipitation of  
193 the precursor and its subsequent washing, the anion used to prepare the precursor had minimal  
194 effect on the final synthesis product. Also, the synthesis protocol included a control of the pH  
195 during the synthesis by an excess of other anions. Therefore, if the pH was not controlled in the  
196 synthesis, the anion could influence the final product. Indeed, Miyawaki et al. (1991) notes  
197 that sulfate and acetate solutions interfered with the formation of kaolinite more than chlorides  
198 and nitrates relating it to the differences in element speciation in solution for these different  
199 solution chemistries. The anions present in the solution during the synthesis of beidellite were  
200 investigated by Kloprogge et al. (1996). One of the experiments consisted of reacting Si-Al gel  
201 at a molar ratio 7.3 : 4.7 with 10 mmol/L salt solution (Na<sub>2</sub>CO<sub>3</sub>, NaOH, NaCl, NaF) at 350 °C  
202 for 10 days at 1 kbar. For samples containing NaCl and Na<sub>2</sub>CO<sub>3</sub> salt solutions pyrophyllite was  
203 reported as main clay mineral phase. For samples containing NaOH, beidellite was reported,  
204 and for sample containing NaF both beidellite and pyrophyllite were reported as products.  
205 Differences in product formation were attributed to the large impact that the different electrolyte  
206 solutions had on the initial pH, which in turn have influence on the final synthesis product.

207 Finally the fourth study by Huve (1992), which discussed the effect of anion on the resulting  
 208 product, emphasizes the presence of F<sup>-</sup> in the reaction medium and its ability to form complexes  
 209 with metals. Indeed, F<sup>-</sup> can play a role on resulting metal complex solubility and element  
 210 coordination state, which in turn can influence further the crystallization of solid phases. Clay  
 211 minerals synthesized using F<sup>-</sup> generally show a higher degree of crystallinity compared to other  
 212 anion salts.

213 **Table 1.** Summary of impurity properties and the general ease to remove them (✓) or not (✗)  
 214 at two different synthesis procedure steps by two different methods.

Impurity properties	Soluble	Soluble	Insoluble	Insoluble
	Low decomposition temperature <600 °C	High decomposition temperature >600 °C	Low decomposition temperature <600 °C	High decomposition temperature >600 °C
Example	NO <sub>3</sub> <sup>-</sup>	SO <sub>4</sub> <sup>2-</sup> (except Ca, Ba, As, Pb); Cl <sup>-</sup> , K <sub>2</sub> CO <sub>3</sub> , Li <sub>2</sub> CO <sub>3</sub> , Na <sub>2</sub> CO <sub>3</sub>	CO <sub>3</sub> <sup>2-</sup> (except Li <sup>+</sup> , Na <sup>+</sup> , Ca <sup>2+</sup> and Ba <sup>2+</sup> )	K <sup>+</sup> , CaSO <sub>4</sub> , BaSO <sub>4</sub> , CaCO <sub>3</sub> , BaCO <sub>3</sub>
Removal after gel precipitation	✓	✓	✓	✗
Removal after synthesis	✓	✓	✓/✗	✗
Removal by heating	✓	✗	✓	✗
Removal by washing	✓	✓	✗	✗

215

### 216 2.2.3. Solution pH during the synthesis

217 The pH conditions of precursor gel or solution that have been reported, range from  
 218 neutral to basic (i.e., from 7 to 10) (Table 2 and 3). Most often the initial pH of the prepared  
 219 reaction mixture was near pH of 8. The adjustment of pH to a specific value is not systematic  
 220 because of the buffering due to formation of the gel precursors. In the studies where it was  
 221 carried out, NaOH or NH<sub>4</sub>OH solutions at various concentrations were used, except in the study

222 of Farmer et al. (1991), where  $\text{Ca}(\text{OH})_2$  was used instead. In the study of Mizutani et al. (1991),  
223 a 5M NaOH solution was used to set  $\text{OH}^-/\text{Fe}$  molar ratio to 7, rather than to adjust the initial  
224 pH to a specific value. The solution pH affects the solubility of solid compounds, the formation  
225 of hydrous gels, and element speciation and activity in the reactive solution. For example,  
226 Doelsch et al. (2001) who studied speciation and crystal chemistry of Fe(III) chloride  
227 hydrolyzed in the presence of  $\text{SiO}_4^{4-}$  found that Si-O-Fe bond is present for samples with  
228  $\text{Si}/\text{Fe} \leq 1$  for the range of pH investigated, but absent for samples prepared at pH = 3 for  
229  $\text{Si}/\text{Fe} = 2$  and  $\text{Si}/\text{Fe} = 4$  and at pH = 5 for  $\text{Si}/\text{Fe} = 4$ . The role of pH on the synthesis of clay  
230 minerals was studied by Baron et al. (2016) and de Kimpe et al. (1961) suggesting that it  
231 influences element speciation in the prepared reaction mixture, which in turn influences the  
232 product obtained during the synthesis. Baron et al. (2016) reported that the increase in synthesis  
233 pH induced the increase of the concentration of anionic aqueous Si species (i.e.,  $\text{H}_3\text{SiO}_4(\text{aq})^-$  and  
234  $\text{H}_2\text{SiO}_4(\text{aq})^{2-}$ ) in the initial solution, and favored the incorporation of Fe(III) in tetrahedral sites  
235 of synthesized nontronites. Frank-Kamenetzkiy et al. (1973) pointed out the effect of initial Al  
236 coordination on the newly formed clay minerals. As such, the aging of Al-Si gels under constant  
237 hydrothermal conditions ( $450\text{ }^\circ\text{C}$ ,  $\text{pH}_2\text{O} = 1000\text{ kg}\cdot\text{cm}^{-2}$ , 3 days), but at different pH, resulted  
238 in the formation of strongly different phases. In acid solutions, pyrophyllite with octahedrally  
239 coordinated  $\text{Al}^{\text{VI}}$ , hydralsite- and andalusite-like phases were formed. In neutral pH, the main  
240 newly formed solid was a random mixed-layer phase of pyrophyllite-beidellite type with both  
241 tetrahedrally and octahedrally coordinated aluminium ( $\text{Al}^{\text{IV}} + \text{Al}^{\text{VI}}$ ) and hydralsite ( $\text{Al}^{\text{VI}}$ ). In  
242 alkaline solution, aluminosilicates nepheline, cancrinite, nosean were formed, possessing only  
243  $\text{Al}^{\text{IV}}$ . The study of Fialips et al. (2000) also reported the effect of pH on synthesized kaolinite  
244 properties. For acidic pH at the end of synthesis a low-defect kaolinite, with high thermal  
245 stability and a hexagonal morphology was obtained, while for the most basic final pH, a high-  
246 defect kaolinite, with low thermal stability and lath shape was found.

247 In practice, pH variation can be important during different synthesis steps, therefore it  
248 is important not to forget to measure the solution pH before and after the synthesis, as well as  
249 the pH of the solutions used during the experiment. In some cases, the solution pH can be very  
250 acidic (close to pH=0) or very basic (close to pH=14), therefore a special care should be taken  
251 to choose the most adapted method to measure the pH.

#### 252 2.2.4. Atmosphere conditions

253 The experiments of 1:1, and in some cases 2:1, iron-rich tri-octahedral clay mineral  
254 synthesis have been carried out under anoxic and/or reducing conditions. Anoxic conditions are  
255 ensured in working in glove box under N<sub>2</sub> or Ar atmosphere, and reducing conditions are  
256 achieved by adding reducing agents such as sodium dithionite Na<sub>2</sub>S<sub>2</sub>O<sub>4</sub> or hydrazine N<sub>2</sub>H<sub>4</sub>  
257 solutions. In the study of Decarreau (1981) the presence of oxygen was limited by bubbling  
258 pure H<sub>2</sub> through the reaction mixture during all synthesis procedure. The reducing and anoxic  
259 conditions ensure that iron is maintained as Fe<sup>2+</sup> during the experiment as it easily oxidizes in  
260 the presence of O<sub>2</sub>. Such conditions are necessary to mimic specific environments (e.g., marine  
261 environment or Mars atmosphere). Other particular conditions during the preparation of  
262 reaction mixture include sea water matrix (Tosca et al., 2016) and addition of F<sup>-</sup> (Boukili et al.,  
263 2015).

#### 264 2.2.5. Synthesis temperature and time

265 Synthesis temperatures vary from 3 °C to 600 °C and last from one day to 3 years.  
266 Temperature, like pH, is expected to influence solubility, activity and speciation of elements in  
267 solution. Furthermore, it also could have effect on crystal germination, nucleation and growth  
268 (Kloprogge et al., 1999). The study of Baker and Strawn (2014) reported an increased cation  
269 ordering in synthetic nontronite samples with increased incubation temperature (up to 150 °C),  
270 in agreement with synthesis reported by Andrieux and Petit (2010), which also note  
271 temperatures up to 150 °C and high pH (around 12) being suitable for the formation of the Fe<sup>3+</sup>-

272 rich smectitic end-member (nontronite). Furthermore, they report that higher temperatures  
273 (200 °C) and lower pH (down to 7) are suitable for the more Al-rich smectites (Fe<sup>3+</sup>-beidellites).  
274 Regarding the influence of time, Grubb (1971) reports that for the same temperature 2:1 type  
275 phase, minnesotaite, becomes dominant over 1:1 type phase for 3-year experiment, while for  
276 the same time minnesotaite is dominant at higher temperatures over 150°C compared to  
277 greenalite.

278         The reactants as well as synthesis conditions (pH, temperature, crystallization times)  
279 and the obtained phases are summarized in Tables 2 and 3. The names of formed IRTOCM  
280 phases have been included as given by the authors.

281 **Table 2.** Summary of 1:1 iron-rich tri-octahedral clay mineral synthesis by hydrothermal method using a gel precursor showing the experimental  
 282 conditions (pH, temperature, aging times) and the neoformed phases.

Publication	Precursor preparation					Aging		Synthesis		Products
	Si source	Fe source	Mg source	pH	Other conditions	Temp., °C	Time	Temp., °C	Time	
Van Hise and Leith (1911)	Na <sub>2</sub> O·3SiO <sub>2</sub>	FeSO <sub>4</sub> or FeCl <sub>2</sub>	soluble Mg <sup>2+</sup> salt	neutral or slightly alkaline	absence of oxygen	-	-	100	n.d.	greenalite
Flaschen and Osborn (1957)	Si(OC <sub>2</sub> H <sub>5</sub> ) <sub>4</sub>	FeCl <sub>2</sub>	-	n.d.	very low oxygen partial pressure	-	-	220 to 470	4 to 14 days	greenalite
Grubb (1971)	4% silica sol prepared from dilute sodium silicate solution	FeCl <sub>2</sub> ·4H <sub>2</sub> O	MgCl <sub>2</sub> ·6H <sub>2</sub> O	5-8	addition of seeding material (magnetite, kaolinite, montmorillonite, albite, quartz)			110-450	2 days to 3 years	crocidolite, greenalite, minnesotaite
Harder (1978)	H <sub>4</sub> SiO <sub>4</sub>	FeSO <sub>4</sub>	Mg(OH) <sub>2</sub>	pH=7-9 (with NaOH)	N <sub>2</sub> atm.; 0.1% Na <sub>2</sub> S <sub>2</sub> O <sub>4</sub> and 0.1% N <sub>2</sub> H <sub>4</sub> ·2HCl			3 and 20	more than 1 day	greenalite and chamosite
Mizutani et al. (1991)	Na <sub>4</sub> SiO <sub>4</sub> ·H <sub>2</sub> O	FeSO <sub>4</sub> ·7H <sub>2</sub> O		pH=3 (with 0.5M H <sub>2</sub> SO <sub>4</sub> ) OH-/Fe=7 (with 5M NaOH)	Na <sub>2</sub> S <sub>2</sub> O <sub>4</sub>	room	1 day	150	50 hours	1:1 iron phyllosilicates
Tosca et al. (2016)	Si(OC <sub>2</sub> H <sub>5</sub> ) <sub>4</sub>	(NH <sub>4</sub> ) <sub>2</sub> Fe <sup>2+</sup> (SO <sub>4</sub> ) <sub>2</sub> ·6H <sub>2</sub> O	-	pH=7; 7.5; 8 (0.1 mM NaOH)	anoxic N <sub>2</sub> /H <sub>2</sub> atm.; seawater matrix	-	-	25	~3 months	greenalite

283



284 **Table 3.** Summary of 2:1 iron-rich tri-octahedral clay mineral synthesis by hydrothermal method using a gel precursor indicating experimental  
 285 conditions (pH, temperature, aging times) and the neoformed phases.

Publication	Preparation of the precursor					Aging		Synthesis		Products
	Si source	Fe source	Mg source	pH	Other	Temp., °C	Time	Temp., °C	Time	
Caillère et al. (1953)	SiO <sub>4</sub> <sup>4-</sup>	Fe <sup>3+</sup> and Fe <sup>2+</sup> salts	Mg <sup>2+</sup> salts	pH=7-9.5 (with NaOH)	HCl, NaCl and KCl	-	-	100	up to 40 days	saponite-like and swelling chlorite-like ferrous phyllosilicates
Roy and Roy (1954)	K <sub>4</sub> SiO <sub>4</sub>	FeNH <sub>4</sub> SO <sub>4</sub>	-	n.d.	-	-	-	300 and 350	up to two weeks	mica-type phase (Fe <sup>3+</sup> muscovite)
Wilkins and Ito (1967)	Na <sub>4</sub> SiO <sub>4</sub>	FeCO <sub>3</sub>	Mg(OH) <sub>2</sub>	pH=8 (with conc. NH <sub>4</sub> OH)	-	120	n.d.	500-550	15-72 hours	talc Mg <sub>52</sub> Fe <sub>48</sub>
Decarreau (1981)	SiO <sub>2</sub> ·Na <sub>2</sub> O	FeCl <sub>2</sub>	MgCl <sub>2</sub>	not adjusted	pure H <sub>2</sub> bubbled through during all synthesis, HCl	-	-	25 and 75	15 days	stevensites and saponites
Farmer et al. (1991)	Si(OC <sub>2</sub> H <sub>5</sub> ) <sub>4</sub>	FeCl <sub>2</sub>	-	pH=8 (with Ca(OH) <sub>2</sub> )	1mM N <sub>2</sub> H <sub>4</sub> , N <sub>2</sub> atm, CaCO <sub>3</sub>	-	-	23 and 89	8 and 12 weeks	saponite and mixed layer saponite-chlorite
Grauby et al. (1994)	Na <sub>2</sub> O·SiO <sub>2</sub> ·5H <sub>2</sub> O	FeCl <sub>3</sub> ·6H <sub>2</sub> O	MgCl <sub>2</sub> ·6H <sub>2</sub> O	pH=9-10 (not adjusted)	-	60	12 hours	200	30 days	nontronite - saponite series
Lantenois et al. (2005)	Si(OC <sub>2</sub> H <sub>5</sub> ) <sub>4</sub>	Fe(NO <sub>3</sub> ) <sub>3</sub> ·9H <sub>2</sub> O	Mg(NO <sub>3</sub> ) <sub>2</sub> ·6H <sub>2</sub> O	pH=6 (with NH <sub>4</sub> OH)	Na <sub>2</sub> CO <sub>3</sub> , ethanol	80	24 hours	400	1 month	SapFe08
Baldermann et al. (2014)	Na <sub>4</sub> SiO <sub>4</sub>	FeSO <sub>4</sub> ·6H <sub>2</sub> O	MgCl <sub>2</sub> ·6H <sub>2</sub> O	pH=8.5 (with NaOH)	Na <sub>2</sub> S <sub>2</sub> O <sub>4</sub>	-	-	60 and 120, and 180	2 and 5, and 7 days	ferrous saponite
Chemtob et al. (2015)	Na <sub>4</sub> SiO <sub>4</sub>	FeCl <sub>2</sub>	MgCl <sub>2</sub> and AlCl <sub>3</sub>	pH=8-9 (not adjusted)	N <sub>2</sub> atm	n.d.	overnight	200	15 days	ferrous smectite
Boukili et al. (2015)	Si(OC <sub>2</sub> H <sub>5</sub> ) <sub>4</sub>	50% as NO <sub>3</sub> <sup>-</sup> and 50% as metallic Fe	-	n.d.	Na <sub>2</sub> CO <sub>3(s)</sub> , AlF <sub>3</sub> or FeF <sub>2</sub>	-	-	600	7 days	trioctahedral micas

286

#### 287 2.2.6. *Microwave-assisted hydrothermal synthesis*

288           There has been recently reported the use of microwave radiation to synthesize Fe<sup>3+</sup>-  
289 saponites (Trujillano et al., 2009). The method is based on hydrothermal synthesis as described  
290 above, but the difference is that the sample is placed in a microwave furnace, where it is  
291 submitted to heat and microwave power at the same time. The microwave power applied causes  
292 heating of the water faster and more efficiently compared to simple heating. Thus higher  
293 temperature and consequently higher pressure inside the reactor can be reached, thus reducing  
294 the rate constant of the reaction. Indeed, the reported reaction time of 8 hours is significantly  
295 shorter than during the usual hydrothermal synthesis.

### 296 **3. Hydrothermal synthesis using a solid precursor**

297           The second group of IRTOCM synthesis comprises the synthesis of IRTOCM from a  
298 template or a previously prepared solid precursor. The summary of studies of IRTOCM using  
299 this synthesis technique is given in Table 4. A large part of the studies included in this section  
300 relates to the research done in the context of nuclear waste disposal, where the interaction  
301 between iron from metallic components and clay from natural or engineered barriers was  
302 investigated. Here, only some publications of these studies reporting the formation of IRTOCM  
303 phases are included. An overview of clay mineral and iron interactions in nuclear waste disposal  
304 conditions can be found in Lantenois et al. (2005), Mosser-Ruck et al. (2010) and the references  
305 herein.

#### 306 *3.1. Solid templates*

307           As a solid precursor for IRTOCM synthesis, FeSi alloy (Flaschen and Osborn, 1957),  
308 glass (Bertoldi et al., 2005) or basalt simulant (Peretyazhko et al., 2016) have been used. In the  
309 series of studies related to the nuclear waste disposal context, the interaction of Callovo -  
310 Oxfordian claystone (COx) with iron is investigated (de Combarieu et al., 2007; Le Pape et al.,

311 2015; Pignatelli et al., 2014; Rivard et al., 2015). COx is mainly composed of clay minerals  
312 (illite, interstratified illite-smectite, chlorite, and kaolinite), with the remaining fraction  
313 consisting of silicates (quartz, K-feldspar, plagioclase, and mica), carbonates (calcite, dolomite,  
314 siderite, and ankerite), pyrite, sulfates, phosphates, and organic matter (Rivard et al., 2015).  
315 Other experimental systems containing solely reference clay minerals such as Wyoming  
316 bentonites (MX80 and Swy-2), natural beidellite (Sbld), nontronite (Garfield) (Herbert et al.,  
317 2016; Lanson et al., 2012; Mosser-Ruck et al., 2016) and kaolinite (KGa-2) (Rivard et al., 2013)  
318 or local bentonites from Slovakia (Osacký et al., 2013) have also been investigated.

319 **Table 4.** Summary of iron-rich 1:1 and 2:1 tri-octahedral clay mineral synthesis by hydrothermal technique using a solid precursor including  
 320 experimental conditions (pH, temperature, aging times) and the neoformed phases.

Publication	Solid	Fe source	Other	Temp., °C	Time	Products
Flaschen and Osborn (1957)	FeSi alloy		very low oxygen partial pressure	220 to 470	4 to 14 days	<i>1:1</i> greenalite
Bertoldi et al. (2005)	glass 3FeO·Al <sub>2</sub> O <sub>3</sub> ·3SiO <sub>2</sub>			575	90 to 214 days	berthierine
de Combarieu et al. (2007)	Callovo–Oxfordian claystone	powdered iron	inert atm.	90	1 to 6 months	Fe-rich silicate from the serpentine group or chlorite
Lanson et al. (2012)	SbId, Swy-2, Garfield nontronite	metallic Fe powder	Ar atm. ; FeSO <sub>4</sub>	80	45 days	Fe-rich serpentines (cronstedtite, odinite)
Osacký et al. (2013)	Bentonites	metallic Fe powder	under air atmosphere	75	35 days	7-Å Fe-phyllsilicate
Rivard et al. (2013)	KGa-2	metallic Fe powder	anoxic atm.; NaCl and CaCl <sub>2</sub> solutions	90	9 months	Fe-rich serpentines of berthierine-greenalite-cronstedtite domain
Pignatelli et al. (2014)	Callovo-Oxfordian claystone	plates of metallic iron and iron powder	inert Ar atm.; NaCl and CaCl <sub>2</sub> solutions; pH = 6.4 at 25 °C	90	6 months	cronstedtite and greenalite
Le Pape et al. (2015)	Callovo-Oxfordian claystone	Fe(0) foil	anoxic atm.; NaCl and CaCl <sub>2</sub> solutions	90	2 months	serpentine 1:1 phyllosilicates
Rivard et al. (2015)	Callovo-Oxfordian claystone	metallic iron	anoxic conditions	90	1,3 and 9 months	serpentine family (odinite, greenalite, berthierine)
Peretyazhko et al. (2016)	Adirondack basalt simulant	FeCl <sub>2</sub>	N <sub>2</sub> atm.; pH=4 (with acetic acid); MgCl <sub>2</sub>	200	1 and 7, and 14 days	<i>2:1</i> Fe(II)-rich saponite
Mosser-Ruck et al. (2016)	MX80 bentonite	metallic Fe and magnetite powder, iron plate	inert Ar atm.; NaCl and CaCl <sub>2</sub> solutions	300	25 months and 9 years	chlorite like minerals or interstratified minerals containing chlorite layers

321

322 *3.2. Iron source*

323 In the studies of Flaschen and Osborn (1957) and Bertoldi et al. (2005) iron is directly  
324 incorporated in the precursor, e.g., in the ferrosilicon alloy or glass melt, respectively. For the  
325 group of studies relating to nuclear waste disposal, iron foil (Le Pape et al., 2015), powder (de  
326 Combarieu et al., 2007; Lanson et al., 2012; Osacký et al., 2013; Rivard et al., 2015, 2013) or  
327 metallic iron plates together with powder (Mosser-Ruck et al., 2016; Pignatelli et al., 2014)  
328 were used. The choice to use iron plates together with powder was due to the fact that the  
329 powder allows a control of corrosion rate and iron input in solution, while the plates allow a  
330 better characterization of alteration products.

331 *3.3. Synthesis conditions*

332 The synthesis in all cases are performed in closed vessels under anoxic conditions. In  
333 some cases, N<sub>2</sub> and Ar gases were used (Lanson et al., 2012; Mosser-Ruck et al., 2016;  
334 Peretyazhko et al., 2016; Pignatelli et al., 2014). For the group of studies relating to nuclear  
335 waste disposal, the medium containing NaCl and CaCl<sub>2</sub> solutions was prepared to approach  
336 realistic on-site conditions in terms of expected solution composition. The synthesis  
337 temperature was 90 °C (de Combarieu et al., 2007; Herbert et al., 2016; Lanson et al., 2012; Le  
338 Pape et al., 2015; Pignatelli et al., 2014; Rivard et al., 2015, 2013) and 300 °C (Mosser-Ruck  
339 et al., 2016). For the other studies, the temperature was in the range 200- 600 °C (Bertoldi et  
340 al., 2005; Flaschen and Osborn, 1957; Peretyazhko et al., 2016). The time for the aging of the  
341 systems is very broad varying from 1 day (Peretyazhko et al., 2016) to 9 years (Mosser-Ruck  
342 et al., 2016).

343 The study of Mosser-Ruck et al. (2010) on the effects of temperature, pH, and iron/clay  
344 and liquid/clay ratios in the context of nuclear waste disposal reported that low temperatures  
345 (<150°C) and large liquid/clay ratios and iron/clay ratios seem to favor the crystallization of the

346 serpentine group minerals instead of Fe-rich trioctahedral smectites or chlorites, the latter being  
347 favored by higher temperatures.

#### 348 **4. Comparison of hydrothermal synthesis techniques using gel or solid** 349 **precursors**

350 As mention researchers in *Handbook of Clay science* (Carrado et al., 2006) “More often  
351 than not, the main objective of producing synthetic clay minerals is to obtain pure samples in a  
352 short time and at the lowest possible temperature.” Furthermore, ideally the steps should be as  
353 less as possible, limiting or simplifying such steps as the preparation of the precursor, its  
354 treatment and the treatment of the product. One would equally wish that the amount and the  
355 state of aggregation allows an easy manipulation of the substances. Thus, based on data reported  
356 in Tables 2, 3 and 4, the choice has been made to compare:

- 357 • synthesis time and temperature;
- 358 • presence/absence of a precursor;
- 359 • number and nature of reactants;
- 360 • nature of obtained products.

##### 361 *4.1. Synthesis time and temperature*

362 The both parameters, time and temperature, are closely related as states the equation of  
363 Arrhenius:

$$364 \quad k = Ae^{\frac{-E_a}{RT}} \quad (\text{Eq.1})$$

365 where  $k$  is the rate constant,  $T$  is the absolute temperature,  $A$  is the pre-exponential  
366 factor,  $E_a$  is the activation energy of the reaction and  $R$  is the universal gas constant. Thus, for  
367 a chemical reaction, the reaction rate constant  $k$  increases with the increase of the temperature  
368  $T$  and/or with the decrease of the activation energy  $E_a$ . For both synthesis approaches, this

369 relation is observed. Experiments performed at lower temperatures (below 100 °C) lasted longer  
370 (several weeks or months) than experiments performed at higher temperatures (above 100 °C),  
371 which were run only for several days. As an example, Tosca et al. (2016) observed the  
372 formation of poorly crystalline greenalite within several weeks of reaction at 25 °C, while  
373 Mizutani et al. (1991) reported the formation of well-crystallized greenalite within two days for  
374 the reaction at 150 °C. In the studies employing use of solid precursor, the experiments at 90 °C  
375 were run during several months to observe the formation of clay minerals (Rivard et al., 2015),  
376 while the experiments performed at 200 °C lasted for 14 days maximum (Peretyazhko et al.,  
377 2016). Although the relation of shorter reaction time for higher temperature during the  
378 experiment is observed for both synthesis approaches, the overall reaction time using gel  
379 precursor is generally less when compared to the use of solid precursor.

#### 380 *4.2. Preparation of precursor*

381 Both approaches require preparation of a precursor. For solid precursor method, the  
382 preparation of a ferrosilicon alloy or glass requires mixing the ingredients and melting them at  
383 elevated temperature (~1400 °C). The preparation of CO<sub>x</sub> or clay minerals requires minimal  
384 effort but clay mineral purification. For gel precursor method, the preparation of an amorphous  
385 gel requires mixing of the reagents, followed by washing and drying of the gel. Such preparation  
386 is more time and effort consuming, but produces more homogenous precursor mixture  
387 (Hamilton and Henderson, 1968). Nevertheless it has to be kept in mind that a certain  
388 heterogeneity due to clustering of elements during different precursor preparation procedures  
389 can occur.

#### 390 *4.3. Reactants*

391 With gel precursor method, every element is introduced by its own chemical compound,  
392 usually in form of salt, whereas in solid precursor method all the necessary elements are

393 introduced together with one solid (ferrosilicon alloy, glass or clay mineral), thus reducing the  
394 number of reactants.

#### 395 *4.4. Synthesized products*

396 The synthesis results vary from one study to another and seem difficult to generalize.  
397 Nevertheless, solid precursor experiments include a wide panel of different minerals and the  
398 discrimination of various kinds of neoformed clay minerals is not always possible. The  
399 experiments using gel precursor also represent different products, but clay minerals remain the  
400 main phase and in some cases it is possible to draw conclusions on the exact clay mineral type.

401 The experiments of IRTOCM synthesis present a wide variety of parameters, which  
402 makes the comparison between the hydrothermal synthesis methods with gel or solid precursor  
403 challenging. For both methods, the synthesis time is similar (not considering studies related to  
404 nuclear waste disposal). The temperature range is also similar, but the synthesis of 1:1 clay  
405 minerals by hydrothermal method using gel precursor seems to be achieved at lower  
406 temperatures. Both methods include different steps to prepare reactants and precursors, with  
407 gel reported to produce homogenous precursor mixture, leading in turn to more homogenous  
408 synthesis products.

## 409 **5. Synthesis conditions and identification of IRTOCM**

### 410 *5.1. 1:1 tri-octahedral clay minerals (serpentine group)*

#### 411 *5.1.1. Common features of synthesis conditions*

412 The 1:1 tri-octahedral Fe-rich clay mineral synthesis reported in the literature were  
413 performed by hydrothermal method using gel precursor (Table 2). This mineral group has also  
414 been reported to form during CO<sub>x</sub> and metallic iron interaction (Table 4). All of these  
415 experiments were performed under anoxic atmosphere (Bertoldi et al., 2005; de Combarieu et  
416 al., 2007; Flaschen and Osborn, 1957; Lanson et al., 2012; Le Pape et al., 2015; Pignatelli et



417 al., 2014; Rivard et al., 2015, 2013; Tosca et al., 2016; Van Hise and Leith, 1911) or in reducing  
418 conditions using such chemicals as sodium dithionite  $\text{Na}_2\text{S}_2\text{O}_4$  (Harder, 1978; Mizutani et al.,  
419 1991). The pH for the reported synthesis was neutral to alkaline. The reactants for precursor  
420 preparation, synthesis temperature and duration were different from one study to another  
421 (discussed previously).

### 422 *5.1.2. Identification and characterization*

423 The identification of the Fe-rich IRTOCM is a challenging exercise requiring the data  
424 from several techniques (Stucki, 2013; Stucki et al., 1989). The main techniques used to  
425 characterize synthesis products are X-ray diffraction (XRD), transmission electron microscopy  
426 (TEM) and Mössbauer spectroscopy. In some cases, Fourier transform infrared spectroscopy  
427 (FTIR) and energy-dispersive X-ray spectroscopy (EDX) coupled to TEM have been used.

428 The early identification of synthesized phases was based on the comparison of  
429 synthesized phases with naturally occurring minerals. Thus, Van Hise and Leith (1911)  
430 identified the ferrous silicate precipitate as greenalite comparing the granular structure and  
431 optical properties of synthesized product with natural rock photomicrograph images. Later,  
432 Flaschen and Osborn (1957) reported the synthesis of greenalite in  $\text{Fe}_x\text{O}_y\text{-SiO}_2\text{-H}_2\text{O}$  system  
433 mentioning that the powder XRD pattern corresponds closely to that of natural greenalite, but  
434 unfortunately no XRD data were included in the publication. Afterwards, in the case of  
435 relatively simple systems, i.e., Si-Fe and Si-Fe-Mg or Si-Fe-Al, powder or oriented XRD  
436 patterns showing approximately 7 Å periodic structure allows to classify the synthesis product  
437 as Fe-rich 1:1 clay mineral (Bertoldi et al., 2005; Harder, 1978; Mizutani et al., 1991; Tosca et  
438 al., 2016). TEM can reveal characteristic hexagonal platelet shape (Mizutani et al., 1991) and  
439 HRTEM confirms 7 Å periodicity (Bertoldi et al., 2005). Mössbauer spectroscopy was used to  
440 obtain information about  $\text{Fe}^{2+}/\text{Fe}^{3+}$  ratio. In the case of the presence of a majority of  $\text{Fe}^{2+}$ , tri-  
441 octahedral structure is suggested (Bertoldi et al., 2005; Mizutani et al., 1991). Furthermore,

442 FTIR identification of  $\text{Fe}^{2+}_3\text{-OH}$  bands in middle infra-red region ( $3625\text{ cm}^{-1}$  stretching and  $653$   
443  $\text{cm}^{-1}$  bending) can support the presence of tri-octahedral character (Fialips et al., 2002; Tosca  
444 et al., 2016). In the case of Si-Fe-Al system, 1:1 tri-octahedral clay minerals can be classified  
445 as berthierine (Bertoldi et al., 2005).

446 For more complex systems, where the four main elements are present, i.e. Si-Fe-Al-Mg,  
447 the identification and classification are even more difficult. The study of Osacký et al. (2013)  
448 have revealed also the interest to use the near infra-red region for the identification of  
449 neoformed phases. Thus, a band near  $4350\text{ cm}^{-1}$  assigned to both  $\text{Fe(II)Mg-OH}$  and  
450  $\text{Fe(II)Fe(II)-OH}$  combination vibrations serves as an additional argument to X-ray diffraction  
451 data to prove the formation of new  $7\text{-\AA}$  Fe-clay mineral phase when changes in middle infra-  
452 red region are not so obvious. Moreover, the assignment of the combination vibrations can be  
453 improved knowing the positions of the OH stretching and bending bands. For example, Gates  
454 (2008) showed, where the bending modes of  $\text{Fe(II)Fe(II)-OH}$  and  $\text{Fe(II)Mg-OH}$  reside. With  
455 these informations, the combination bands could be better identified and assigned. In the case  
456 of the studies related to the interaction of  $\text{CO}_x$  with metallic Fe, the early studies of this system  
457 (de Combarieu et al., 2007), coupled XRD and scanning electron microscopy (SEM) to  
458 conclude that Fe-rich silicate from the serpentine group or chlorite have been formed. Further  
459 more detailed studies including the characterization by FTIR, TEM-EDX and Mössbauer  
460 spectroscopy revealed the heterogeneity of the newly precipitated phases belonging to 1:1 clay  
461 mineral serpentine group odinite-greenalite-berthierine domain (Le Pape et al., 2015; Rivard et  
462 al., 2015). A thorough study of materials by X-ray spectroscopy evidences as well the mixture  
463 of starting solid phase (kaolinite in this study) and Fe-serpentine layers of berthierine-  
464 greenalite-cronstedtite (Rivard et al., 2013). The combined use of TEM-EDS and scanning  
465 transmission X-ray microscopy (STXM) results had allowed to quantify the percentage of  
466 berthierine and cronstedtite-greenalite type minerals in the analyzed material. For two other

467 studies, the thorough characterization indicated that the obtained phases fall close to  
468 cronstedtite and greenalite (Pignatelli et al., 2014) or cronstedtite and odinite-type minerals  
469 (Lanson et al., 2012).

## 470 5.2. 2:1 tri-octahedral clay minerals (saponite group)

### 471 5.2.1. Common features of synthesis conditions

472 The 2:1 IRTOCM synthesis was mainly performed by hydrothermal method using a gel  
473 precursor (Baldermann et al., 2014; Chemtob et al., 2015; Decarreau, 1981; Farmer et al., 1991;  
474 Grauby et al., 1994; Lantenois et al., 2005; Wilkins and Ito, 1967), except the studies of  
475 Trujillano et al. (2009), Caillère et al. (1953) and Peretyazhko et al. (2016). Trujillano et al.  
476 (2009) had reported the preparation of Fe<sup>3+</sup>-saponite by hydrothermal synthesis assisted by  
477 microwave radiation. Caillère et al. (1953) reported the synthesis of saponite-like and swelling  
478 chlorite-like ferrous clay minerals by precipitation of solid at boiling temperature. The  
479 occurrence of Fe(II)-rich saponite was reported by Peretyazhko et al. (2016) reacting solid  
480 (basalt simulant) with FeCl<sub>2</sub> solution. From the series of studies related to the context of nuclear  
481 waste disposal, Herbert et al. (2016) had identified different 1:1 and 2:1 tri-octahedral mineral  
482 interstratifications such as cronstedtite-saponite-trioctahedral vermiculite, berthierine-saponite  
483 and chlorite-saponite-trioctahedral vermiculite among other phases.

484 To synthesize 2:1 IRTOCM with hydrothermal method using a gel precursor, TEOS or  
485 sodium silicate have been used as source of Si (Table 3). The sources of Fe and Mg are various  
486 including chlorides, sulfates, nitrates and carbonates. The pH of the solution after the precursor  
487 precipitation had been reported to be basic in most cases. Acidic pH has been reported in the  
488 study of Lantenois et al. (2005) (pH=6) and Peretyazhko et al. (2016) (pH=4). Some, but not  
489 all, studies report using inert or oxygen-poor atmosphere conditions (Chemtob et al., 2015;  
490 Decarreau, 1981; Farmer et al., 1991; Peretyazhko et al., 2016). In the study of Baldermann et  
491 al. (2014), reducing conditions were ensured by adding sodium dithionite to reactants. The

492 aging of precursor is not systematic and reported in three cases (Grauby et al., 1994; Lantenois  
493 et al., 2005; Wilkins and Ito, 1967) for the temperature range of 60 °C to 120 °C and over  
494 durations of 12 to 24 hours. The reported range of synthesis temperatures is large varying from  
495 23 °C to 600 °C (Table 3). The synthesis time of 2:1 IRTOCM was reported from 1 day to 2  
496 months (Table 3), which is though shorter compared to 1:1 IRTOCM synthesis, where  
497 experiments are reported to last up to 9 months.

#### 498 *5.2.2. Identification and characterization*

499 Early studies of 2:1 IRTOCM used XRD and FTIR to characterize synthesis products  
500 (Caillère et al., 1953; Decarreau, 1981; Farmer et al., 1991; Wilkins and Ito, 1967), but owing  
501 to their time the publications included only limited examples of XRD or FTIR spectroscopy  
502 experimental data. Fortunately, the subsequent work could benefit accommodating more  
503 experimental data in the publications. Routine powder XRD analysis coupled with FTIR  
504 spectroscopy allows the identification of type of neoformed clay mineral phase and to check  
505 the presence or absence of impurities (Boukili et al., 2015; Chemtob et al., 2015; Grauby et al.,  
506 1994; Lantenois et al., 2005; Peretyazhko et al., 2016; Trujillano et al., 2009). Different  
507 treatments of oriented preparations of XRD slides (saturation with Ca, K, ethylene glycol and  
508 heating to 500 °C) have potential identifying interstratified phases (Farmer et al., 1991).  
509 Nevertheless, the XRD along with FTIR spectroscopy both remain bulk analysis for clay  
510 mineral structure identification. There could be several reasons for the broadness of diffraction  
511 peaks such as the aforementioned interstratification or poor crystallinity. The analysis of  
512 separate particles using TEM or high-resolution TEM can bring clarification to these points,  
513 but the sample representativeness is largely reduced (Baldermann et al., 2014; Inoué and  
514 Kogure, 2016). It can be overcome to some extent with large number of analysis. Recently  
515 Chemtob et al. (2015) used X-ray absorption spectroscopy (XAS) methods to provide a  
516 supplementary proof of tri-octahedral character of neoformed iron-saponite phases.

517 The chemical analysis of synthesis products have been determined by electron  
518 microprobe analysis (Lantenois et al., 2005; Peretyazhko et al., 2016), inductively coupled  
519 plasma optical emission spectrometry (ICP-OES) (Chemtob et al., 2015) and analytical electron  
520 microscopy (AEM) (Baldermann et al., 2014; Grauby et al., 1994). In the case of pure clay  
521 minerals obtained, bulk sample analysis such as ICP-OES and Mössbauer spectroscopy can be  
522 considered to establish sample stoichiometry (Chemtob et al., 2015). On the other hand, single  
523 particle analysis can potentially evidence the chemical heterogeneity of sample (Grauby et al.,  
524 1994), but require sufficient amount of data to be statistically representative. In the studies,  
525 where several crystalline phases were identified, single particle analysis by energy dispersive  
526 X-ray spectroscopy (EDX) and electron energy loss spectroscopy (EELS) can be more relevant  
527 (Baldermann et al., 2014).

### 528 *5.3. Chlorites*

#### 529 *5.3.1. Common features of synthesis conditions*

530 The synthesis of iron-rich tri-octahedral chlorite (chamosite) has been reported by  
531 Harder (1978) and Mosser-Ruck et al. (2016). In both cases, chamosite is reported occurring  
532 with other clay minerals, also as an interstratified phase. The synthesis experiments have been  
533 described in previous sections. For the series of experiments related to the nuclear waste  
534 disposal (Mosser-Ruck et al., 2010) on the effects of temperature, it was found that low  
535 temperatures (<150°C) seem to favor the crystallization of the serpentine group minerals, while  
536 higher temperatures favor the formation of Fe-rich trioctahedral smectites or chlorites.  
537 Nevertheless, Harder (1978) reported the formation of chlorite in the temperature as low as  
538 20 °C, but as discussed previously the limits to include the experimental data in older  
539 publications does not allow the interpretation of data today. In geological systems, different  
540 range of temperatures for chlorite formation have been distinguished (Beaufort et al., 2015). Its  
541 formation temperature is near 200 °C in hydrothermal systems, but in diagenetic systems Fe

542 chlorite is reported to form in 40 °C-120 °C range. Such difference was attributed to different  
543 heating rates, heat-flow conditions and pressure.

### 544 *5.3.2. Identification and characterization*

545 The same characterization techniques as described previously for 1:1 and 2:1 clay  
546 minerals have been used identifying chamosite. As it often occurs as interstratified phase and  
547 has different polytypes, great care has been taken to consider and to study these aspects by XRD  
548 (Bailey, 1988; Reynolds et al., 1992) and HRTEM (Inoué and Kogure, 2016).

## 549 **6. Geochemical simulation using thermodynamic properties of IRTOCM**

550 One of the interests in the study of synthesis or IRTOCM is their incorporation in  
551 geochemical simulations in order to predict long-term stability of certain geological formations.  
552 Clay minerals have a wide variety of isomorphic substitutions, they occur as mixed-layer phases  
553 and have small particle size usually less than 2µm. This structural and chemical complexity  
554 makes it difficult to introduce them in such simulations. Nevertheless, several numerical  
555 approaches have been developed for the estimation of thermodynamic properties of clay  
556 minerals (Chen, 1975; Chermak and Rimstidt, 1989; Nriagu, 1975; Sposito, 1986; Tardy and  
557 Fritz, 1981; Tardy and Garrels, 1974; Vieillard, 2000, 1994) and introduced in different  
558 databases such as Thermoddem (Blanc et al., 2012) or LLNL (Johnson et al., 2000). These  
559 databases are particularly useful when applied in geochemical simulation codes such as  
560 PHREEQC (Parkhurst and Appelo, 2013) or Geochemist's Workbench® (Bethke, 2007)  
561 among others to simulate various systems.

562 Three approaches can be distinguished for the estimation of thermodynamic properties  
563 of clay minerals. First approach, consists of the summation of respective oxyde and/or  
564 hydroxyde parameters using "polyhedral summation" (Chermak and Rimstidt, 1989; Nriagu,  
565 1975; Sposito, 1986; Tardy and Garrels, 1974), "regression" (Chen, 1975) or "electronegativity

566 differences of cations” (Vieillard, 2000, 1994) techniques. Second approach is based on the  
567 ideal mixing of end-member clays (Tardy and Fritz, 1981) and the third approach uses the data  
568 of ionic species for the estimation of thermodynamic properties (Eugster and Chou, 1973). The  
569 last approach is limited to a particular case, where a direct precipitation of solid from solution  
570 occurs. As no direct measurements of IRTOCM thermodynamic properties have been  
571 performed, the application of second approach is also limited. Therefore, in studies, where  
572 simulations involving IRTOCM were performed, the first approach (summation of  
573 oxyde/hydroxyde parameters) has been used (Chevrier et al., 2007; Halevy et al., 2017; Zolotov,  
574 2015), because the thermodynamic properties of oxydes and hydroxydes are rather well known  
575 (Snow et al., 2011, 2010a, 2010b; Stølen et al., 1996).

576         Two recent studies have dealt with the confrontation of the experimentally observed  
577 formation of iron-rich tri-octahedral clay minerals and the data issued from geochemical  
578 simulation (Pignatelli et al., 2013; Wilson et al., 2015). The experiments performed by Wilson  
579 et al. (2015) estimated montmorillonite stability in contact with iron. In this study the polyhedral  
580 summation technique of clay mineral constituting oxides and hydroxides were used to obtain  
581 their thermodynamic properties (Helgeson et al., 1978; Holland, 1989). The study revealed that  
582 experimentally detected phases were in agreement with simulations. Another experiment of  
583 Pignatelli et al. (2013) used a database Thermoddem (Blanc et al., 2012) (which includes the  
584 approach of Vieillard (2000, 1994) on oxyde summation based on the electronegativity  
585 differences of cations). In this study (Pignatelli et al., 2014) the stability field of cronstedtite  
586 was calculated and confronted with the data of their experimental observations. They note that  
587 below 50°C cronstedtite is predicted to be more stable than what it is observed and this  
588 difference was attributed to the various polytypes of mineral which is not taken into account in  
589 the calculations of Veillard’s approach. Moreover, to explain the presence of several phases  
590 instead of one as predicted by geochemical simulations, they suggest a reaction path with local

591 changes in Fe concentration. Two aforementioned experiments deal with rather complex  
592 systems, and have allowed to compare the formation of one or several particular mineral phases  
593 at given experimental conditions.

594         A recent study of Tosca et al. (2016) focused on single IRTOCM, greenalite, formation  
595 conditions by direct precipitation. To compare the obtained mineral thermodynamic properties  
596 with the literature, they performed solubility experiment, thus obtaining information about the  
597 equilibrium constant of the reaction. The obtained experimental values were compared with the  
598 data calculated by Eugster and Chou (1973) and agrees rather well. The difference is attributed  
599 to the fact that clays are particles of finite size, while in thermodynamics the assumption is  
600 made that the phase is infinite. Important that they note to be in thermodynamic equilibrium  
601 conditions, where the formation of other metastable phases can be omitted.

602         Although the experiment of Tosca et al. (2016) was performed at equilibrium  
603 conditions, in practice such conditions are difficult to achieve or impossible to demonstrate  
604 especially for more complex systems such as in the studies of Wilson et al. (2015) and  
605 Pignatelli et al. (2013). Thus, the experiments (unsteady state) performed are compared with  
606 calculations obtained from a thermodynamic equilibrium (steady state). Even though, the  
607 formation of a mineral or its dissolution can be predicted to occur under given conditions, these  
608 processes could be negligible because their rate is very slow. For this reason, kinetic evaluations  
609 should be also considered. Recently numerical models involving nucleation and crystal growth  
610 have been developed, which take into account the change occurring in the system (time  
611 dependence) (Noguera et al., 2006a). Such model can be compared with experimental results  
612 because the operating conditions are close to the modelling hypothesis. In perspective, it would  
613 be interesting to confront these calculations with experimental observations of the formation of  
614 iron-rich tri-octahedral clay minerals.

## 615 **7. Iron (III) and aluminium configuration and distribution**



616           Apart from geochemical simulations, other interest in IRTOCM synthesis lays in the  
617 possibility to control the synthesized phases chemistry and structure, which in turn can give  
618 information about the formation conditions of such phases in natural environments. Most  
619 common elements possible to constitute IRTOCM are Si, Mg, Al and Fe. M(II) such as Mg and  
620 Fe(II) and M(IV) such as Si can enter only octahedral and tetrahedral sites in clay mineral  
621 structure only, respectively, but M(III) such as Al and Fe(III) can be found in both, in tetrahedral  
622 and octahedral sheets in different proportions. Recent studies link this feature to the element  
623 speciation in the reactant solution (Baron et al., 2016). Thus, Pokrovski et al. (2003) have shown  
624 that in Si-free solution Fe(III) adopts octahedral coordination whereas in the presence of Si, a  
625 portion of Fe(III) is found to be tetrahedrally coordinated. The experiments performed by Baron  
626 et al. (2016), indeed show an increase of tetrahedrally coordinated Fe(III) in synthesized  
627 nontronites in function of different Si species in solution, which in turn depend on pH.

628           In the same experiments performed by Pokrovski et al. (2003), they note that the presence  
629 of Si in the solution favors the formation of Fe-Si linkages. If we assume the hypothesis that  
630 the IRTOCM formation occurs similarly as suggested for other clay minerals first by the  
631 precipitation of octahedral sheet, followed by the formation of tetrahedral sheet (Carrado et al.,  
632 2000; Huertas et al., 2000), then M(II) and M(III) octahedral coordination in solution or  
633 polymerized hydroxide complexes would be determinant. However, as showed by Pokrovski et  
634 al. (2003) presence of aqueous Si inhibit Fe(III) polymerization and thus solid-phase formation.  
635 An earlier study on Si effect on Ga complexes (which can be considered similar to aluminium  
636 ones) shows similar trend, in the fact that in the presence of Si in solution Ga adopts tetrahedral  
637 coordination and Ga-Si complexes are formed Pokrovski et al. (2002). The formation of such  
638 complexes M(III)-Si in solution could then explain the facility to form homogenous gels, but  
639 difficulty to obtain crystalline structures as observed by de Kimpe et al. (1961) and Hem et al.  
640 (1973).

641 It has to be noted that the studies about element speciation in solution have been  
642 performed in diluted solutions and at ambient conditions, while the preparation of clay mineral  
643 precursors often is performed at concentrated solutions and the synthesis is carried out at  
644 hydrothermal conditions. In perspective, it would be interesting to investigate the element  
645 speciation and their synergistic effects at concentrated solutions and at elevated temperature  
646 and pressure.

## 647 **8. Conclusion**

648 Iron-rich tri-octahedral clay minerals have been identified occurring on the surface of  
649 Mars, in meteorites, deep-sea environment, subduction zones and transform faulting. The  
650 formation conditions of these clay minerals have not yet been fully understood. Moreover, the  
651 thermodynamic constants of these minerals are scarce, which does not allow to predict their  
652 stability in long term. This aspect is important for nuclear waste disposal sites, where the  
653 formation of iron-rich clay minerals have been observed on steel and clay-rich rock interface  
654 or at the interface between iron and silica glass. These minerals could also have a potential to  
655 be used as heterogeneous catalysts. In order to obtain sufficient amount of such minerals for  
656 further thermodynamic studies and to investigate their formation conditions, the synthesis of a  
657 series of iron-rich tri-octahedral clay minerals with different Si/Fe molar ratio is necessary. This  
658 study reviews the previously reported methods and conditions for iron-rich tri-octahedral clay  
659 mineral synthesis. Two different approaches have been used to hydrothermally synthesize iron-  
660 rich tri-octahedral minerals : using gel or solid precursor. The synthesis of 1:1 type clay minerals  
661 were performed in reducing conditions in neutral or alkaline pH. The parameters for 2:1 type  
662 clay minerals synthesis was in most cases similar to 1:1 type clay mineral synthesis, but  
663 included also acidic pH and oxidizing conditions.

664 Previous synthesis of iron-rich tri-octahedral clay mineral phases have not been  
665 systematic, because the studies were focused on particular geological or application question.  
666 Therefore, in future, it could be interesting to investigate in the systematic manner the optimum  
667 synthesis conditions (nature and ratio of reactants, pH, temperature, time and water amount)  
668 starting from the simplest of the systems Si-Fe(II). The characterization of neoformed products  
669 should include powder X-ray diffraction, X-ray diffraction of oriented films (air-dried and  
670 saturated with ethylene glycol), FTIR and Mössbauer spectroscopies, as well as TEM.

671 In perspective, two areas of studies seem particularly interesting for further  
672 investigation: (1) the confrontation of experimental and geochemical simulation data, and (2)  
673 the effect of element speciation in solution on the chemical composition of the neoformed solid.  
674 Recently, a numerical simulation accounting for the processes of nucleation, growth,  
675 dissolution and ageing of particles in an initially supersaturated closed system was developed  
676 (Noguera et al., 2006a, b). It could then be interesting to observe the nucleation and crystal  
677 growth in Si-Fe system in real time in-situ and confront the obtained results with the  
678 simulations. The influence of a parameter such as the pH, its role on element speciation in  
679 solution and their subsequent effect on crystal growth and nucleation could be assessed.

## 680 **Acknowledgments**

681 We are grateful to two anonymous reviewers for their comments and suggestions, and Fabien  
682 Baron for his comments, suggestions and discussions, which have significantly improved the  
683 manuscript.

684 **References**

- 685 Andrieux, P., Petit, S., 2010. Hydrothermal synthesis of dioctahedral smectites: The Al-Fe<sup>3+</sup>  
686 chemical series. Part I: Influence of experimental conditions. *Appl. Clay Sci.* 48, 5–17.  
687 <https://doi.org/10.1016/j.clay.2009.11.019>
- 688 Arundhathi, R., Sreedhar, B., Parthasarathy, G., 2011. Highly efficient heterogenous catalyst  
689 for O-arylation of phenols with aryl halides using natural ferrous chamosite. *Appl. Clay*  
690 *Sci.* 51, 131–137. <https://doi.org/10.1016/j.clay.2010.11.014>
- 691 Arundhathi, R., Sreedhar, B., Parthasarathy, G., 2010. Chamosite, a naturally occurring clay as  
692 a versatile catalyst for various organic transformations. *Clay Miner.* 45, 281–299.  
693 <https://doi.org/10.1180/claymin.2010.045.3.281>
- 694 Bailey, S.W., 1988. X-ray diffraction identification of the polytypes of mica, serpentine, and  
695 chlorite. *Clays Clay Miner.* 36, 193 LP-213.
- 696 Baker, L.L., Strawn, D.G., 2014. Temperature Effects on the Crystallinity of Synthetic  
697 Nontronite and Implications for Nontronite Formation in Columbia River Basalts. *Clays*  
698 *Clay Miner.* 62, 89 LP-101.
- 699 Baldermann, A., Dohrmann, R., Kaufhold, S., Nickel, C., Letofsky-Papst, I., Dietzel, M., 2014.  
700 The Fe-Mg-saponite solid solution series a hydrothermal synthesis study. *Clay Miner.* 49,  
701 391–415. <https://doi.org/10.1180/claymin.2014.049.3.04>
- 702 Baldermann, A., Dohrmann, R., Kaufhold, S., Nickel, C., Letofsky-Papst, I., Dietzel, M., 2014.  
703 The Fe-Mg-saponite solid solution series – a hydrothermal synthesis study. *Clay Miner.*  
704 49, 391–415.
- 705 Baldermann, A., Warr, L.N., Letofsky-Papst, I., Mavromatis, V., 2015. Substantial iron  
706 sequestration during green-clay authigenesis in modern deep-sea sediments. *Nat. Geosci.*

707 8, 3–8. <https://doi.org/10.1038/ngeo2542>

708 Baron, F., 2016. Thesis. Le fer dans les smectites : une approche par synthèses minérales.  
709 Université de Poitiers (France).

710 Baron, F., Petit, S., Tertre, E., Decarreau, A., 2016. Influence of Aqueous Si and Fe Speciation  
711 on Tetrahedral Fe(III) Substitutions in Nontronites: a Clay Synthesis Approach. *Clays*  
712 *Clay Miner.* 64, 230–244. <https://doi.org/10.1346/CCMN.2016.0640309>

713 Beaufort, D., Rigault, C., Billon, S., Billault, V., Inoue, A., Inoue, S., Patrier, P., 2015. Chlorite  
714 and chloritization processes through mixed-layer mineral series in low-temperature  
715 geological systems – a review. *Clay Miner.* 50, 497–523.  
716 <https://doi.org/10.1180/claymin.2015.050.4.06>

717 Bertoldi, C., Dachs, E., Cemic, L., Theye, T., Wirth, R., Groger, W., 2005. The Heat Capacity  
718 of the Serpentine Subgroup Mineral Berthierine (Fe<sub>2.5</sub>Al<sub>0.5</sub>)[Si<sub>1.5</sub>Al<sub>0.5</sub>O<sub>5</sub>](OH)<sub>4</sub>. *Clays*  
719 *Clay Miner.* 53, 380 LP-388.

720 Bethke, C.M., 2007. *Geochemical and Biogeochemical Reaction Modeling*. Cambridge  
721 University Press, Cambridge. <https://doi.org/10.1017/CBO9780511619670>

722 Blanc, P., Lassin, A., Piantone, P., Azaroual, M., Jacquemet, N., Fabbri, A., Gaucher, E.C.,  
723 2012. Thermoddem: A geochemical database focused on low temperature water/rock  
724 interactions and waste materials. *Appl. Geochemistry* 27, 2107–2116.  
725 <https://doi.org/10.1016/j.apgeochem.2012.06.002>

726 Boukili, B., El Moutaouakkil, N., Robert, J.-L., Meunier, A., Ventura, G.D., 2015.  
727 Experimental investigation of trioctahedral micas in the Na<sub>2</sub>O-FeO-Fe<sub>2</sub>O<sub>3</sub>-Al<sub>2</sub>O<sub>3</sub>-SiO<sub>2</sub>-  
728 H<sub>2</sub>O-HF system. *J. Mater. Environ. Sci.* 6, 2917–2928.

729 Bourg, I.C., 2015. Sealing Shales versus Brittle Shales: A Sharp Threshold in the Material  
730 Properties and Energy Technology Uses of Fine-Grained Sedimentary Rocks. *Environ.*  
731 *Sci. Technol. Lett.* 2, 255–259. <https://doi.org/10.1021/acs.estlett.5b00233>

732 Caillère, S., Henin, S., Esquevin, J., 1953. Synthèses à basse température de phyllite ferrifère.  
733 *Comptes Rendus l'Academie Sci.* 237, 1724–1726.

734 Carrado, K.A., Decareau, A., Petit, S., Bergaya, F., Lagaly, G., 2006. Synthetic clay minerals  
735 and purification of natural clays, in: Bergaya, F., Theng, B.K.G., Lagaly, G. (Eds.),  
736 *Handbook of Clay Science*. Elsevier Ltd, 115–139. [https://doi.org/10.1016/S1572-](https://doi.org/10.1016/S1572-4352(05)01004-4)  
737 [4352\(05\)01004-4](https://doi.org/10.1016/S1572-4352(05)01004-4)

738 Carrado, K.A., Xu, L., Gregory, D.M., Song, K., Seifert, S., Botto, R.E., 2000. Crystallization  
739 of a layered silicate clay as monitored by small-angle X-ray scattering and NMR. *Chem.*  
740 *Mater.* 12, 3052–3059. <https://doi.org/10.1021/cm000366a>

741 Chemtob, S.M., Nickerson, R.D., Morris, R. V., Agresti, D.G., Catalano, J.G., 2015. Synthesis  
742 and structural characterization of ferrous trioctahedral smectites: Implications for clay  
743 mineral genesis and detectability on Mars. *J. Geophys. Res. Planets* 120, 1119–1140.  
744 <https://doi.org/10.1002/2014JE004763>

745 Chen, C.-H., 1975. A method of estimation of standard free energies of formation of silicate  
746 minerals at 298.15 degrees K. *Am. J. Sci.* 275, 801–817.  
747 <https://doi.org/10.2475/ajs.275.7.801>

748 Chermak, J.A., Rimstidt, J.D., 1989. Estimating the thermodynamic properties ( $\Delta G$  of and  
749  $\Delta H$  of ) of silicate minerals at 298 K from the sum of polyhedral contributions. *Am.*  
750 *Mineral.* 74, 1023–1031.

751 Chevrier, V., Poulet, F., Bibring, J., 2007. Early geochemical environment of Mars as

752 determined from thermodynamics of phyllosilicates. *Nature* 448, 2–5.  
753 <https://doi.org/10.1038/nature05961>

754 de Combarieu, G., Barboux, P., Minet, Y., 2007. Iron corrosion in Callovo-Oxfordian argilite:  
755 From experiments to thermodynamic/kinetic modelling. *Phys. Chem. Earth* 32, 346–358.  
756 <https://doi.org/10.1016/j.pce.2006.04.019>

757 de Kimpe, C., Gastuche, M.C., Brindley, G., 1961. Ionic coordination in alumino-silicic gels  
758 in relation to clay mineral formation. *Am. Mineral.* 46, 1370–1381.

759 Decarreau, A., 1981. Cristallogénèse à basse température de smectites trioctaédriques par  
760 vieillissement de coprécipités silicométalliques. *Comptes rendus des séances l'Académie*  
761 *des Sci.* 292, 61–64.

762 Doelsch, E., Stone, W.E.E., Petit, S., Masion, A., 2001. Speciation and Crystal Chemistry of  
763 Fe ( III ) Chloride Hydrolyzed in the Presence of SiO<sub>4</sub> Ligands . 2 . Characterization of  
764 Si - Fe Aggregates by FTIR and <sup>29</sup> Si Solid-State NMR 1399–1405.

765 Dzene, L., 2016. Thesis. Influence of particle size and crystal chemistry on cation exchange  
766 properties of swelling clay minerals. Université de Poitiers (France).

767 Eugster, H.P., Chou, I.-M., 1973. The Depositional Environments of Precambrian Banded Iron-  
768 Formations. *Econ. Geol.* 68, 1144–1168.

769 Farmer, V.C., Krishnamurti, G.S.R., Htjang, A.P.M., 1991. Synthetic Allophane and Layer-  
770 Silicate Formation in SiO<sub>2</sub>-Al<sub>2</sub>O<sub>3</sub>-FeO-Fe<sub>2</sub>O<sub>3</sub>-MgO-H<sub>2</sub>O Systems at 23 and 89 C in a  
771 Calcareous Environment. *Clays Clay Miner.* 39, 561–570.

772 Feuillie, C., Daniel, I., Michot, L.J., Pedreira-Segade, U., 2013. Adsorption of nucleotides onto  
773 Fe-Mg-Al rich swelling clays. *Geochim. Cosmochim. Acta* 120, 97–108.

774 <https://doi.org/10.1016/j.gca.2013.06.021>

775 Fialips, C.-I., Huo, D., Yan, L., Wu, J., Stucki, J.W., 2002. Effect of Fe oxidation state on the  
776 IR spectra of Garfield nontronite. *Am. Mineral.* 87, 630-641.

777 Fialips, C.I., Petit, S., Decarreau, A., Beaufort, D., 2000. Influence of synthesis pH on kaolinite  
778 “crystallinity” and surface properties. *Clays Clay Miner.* 48, 173–184.  
779 <https://doi.org/10.1346/CCMN.2000.0480203>

780 Flaschen, S.S., Osborn, E.F., 1957. Studies of the system iron oxide-silicawater at low oxygen  
781 partial pressures. *Econ. Geol.* 52, 923–943. <https://doi.org/10.2113/gsecongeo.52.8.923>

782 Frank-Kamenetzkiy, V.A., Kotov, N. V, Tomashenko, A.N., 1973. The role of AlIV and AlVI  
783 in transformation and synthesis of layer silicates. *Krist. und Tech.* 8, 425–435.  
784 <https://doi.org/10.1002/crat.19730080404>

785 Garrido-Ramírez, E.G., Theng, B.K.G., Mora, M.L., 2010. Clays and oxide minerals as  
786 catalysts and nanocatalysts in Fenton-like reactions - A review. *Appl. Clay Sci.* 47, 182–  
787 192. <https://doi.org/10.1016/j.clay.2009.11.044>

788 Gates, W.P., 2008. Cation mass-valence sum (CM-VS) approach to assigning OH-bending  
789 bands in dioctahedral smectites. *Clays Clay Miner.* 56, 10–22.  
790 <https://doi.org/10.1346/CCMN.2008.0560102>

791 Grambow, B., 2016. Geological Disposal of Radioactive Waste in Clay. *Elements* 12, 239–245.  
792 <https://doi.org/10.2113/gselements.12.4.239>

793 Grauby, O., Petit, S., Decarreau, A., Baronnet, A., 1994. The nontronite-saponite series: an  
794 experimental approach. *Eur. J. Mineral.* 6, 99–112.

795 Grubb, P.L.C., 1971. Silicates and their paragenesis in the brockman iron formation of



796 Wittenoom Gorge, Western Australia. *Econ. Geol.* 66, 281–292.  
797 <https://doi.org/10.2113/gsecongeo.66.2.281>

798 Halevy, I., Alesker, M., Schuster, E.M., Popovitz-Biro, R., Feldman, Y., 2017. A key role for  
799 green rust in the Precambrian oceans and the genesis of iron formations. *Nat. Geosci.* 10,  
800 135–139. <https://doi.org/10.1038/ngeo2878>

801 Hamilton, D.L., Henderson, C.M.B., 1968. The preparation of silicate compositions by a gelling  
802 method. *Mineral. Mag.* 36, 832–838. <https://doi.org/10.1180/minmag.1968.036.282.11>

803 Harder, H., 1978. Synthesis of Iron Layer Silicate Minerals. *Clays Clay Miner.* 26, 65–72.  
804 <https://doi.org/10.1346/CCMN.1978.0260108>

805 Helgeson, H.C., Delany, J.M., Nesbitt, H.W., Bird, D.K., 1978. Summary and Critique of the  
806 Thermodynamic Properties of Rock-Forming Minerals. Yale University. Kline Geology  
807 Laboratory.

808 Hem, J.D., Roberson, C.E., Lind, C.J., Polzer, W.L., 1973. Chemical Interactions of Aluminum  
809 with Aqueous Silica at 25°C. Geological Survey Water-Supply Paper 1827-E.

810 Herbert, H.-J., Kasbohm, J., Nguyen-Thanh, L., Meyer, L., Hoang-Minh, T., Xie, M.,  
811 Mählmann, R.F., 2016. Alteration of expandable clays by reaction with iron while being  
812 percolated by high brine solutions. *Appl. Clay Sci.* 121–122, 174–187.  
813 <https://doi.org/10.1016/j.clay.2015.12.022>

814 Holland, T.J.B., 1989. Dependence of entropy on volume for silicate and oxide minerals; a  
815 review and predictive model. *Am. Mineral.* 74, 5–13.

816 Huertas, F.J., Cuadros, J., Huertas, F., Linares, J., 2000. Experimental study of the hydrothermal  
817 formation of smectite in the Beidellite-Saponite series. *Am. J. Sci.*

818 <https://doi.org/10.2475/ajs.300.6.504>

819 Huve, L., 1992. Thesi. Synthèse de phyllosilicates en milieu acide et fluoré et leur  
820 caractérisation. Université de Haute-Alsace (France).

821 Inoué, S., Kogure, T., 2016. High-resolution transmission electron microscopy (HRTEM) study  
822 of stacking irregularity in fe-rich chlorite from selected hydrothermal ore deposits. *Clays  
823 Clay Miner.* 64, 131–144. <https://doi.org/10.1346/CCMN.2016.0640205>

824 Jaber, M., Komarneni, S., Zhou, C.-H., 2013. Synthesis of Clay Minerals, in: Bergaya, F.,  
825 Lagaly, G. (Eds.), *Handbook of Clay Science Fundamentals*. Elsevier, pp. 223–241.  
826 <https://doi.org/10.1016/B978-0-08-098258-8.00009-2>

827 Johnson, J., Anderson, F., Parkhurst, D., 2000. Database thermo.com.V8.R6.230, Rev 1.11.

828 Klopogge, J.T., Komarneni, S., Amonette, J.E., 1999. Synthesis of smectite clay minerals: A  
829 critical review. *Clays Clay Miner.* 47, 529–554.  
830 <https://doi.org/10.1346/CCMN.1999.0470501>

831 Klopogge, J.T., Vogels, R.J.M.J., Van Der Eerden, A.M.J., 1996. Hydrothermal synthesis of  
832 pyrophyllite from Si-Al gels and salt solutions: Some implications for the formation of  
833 pyrophyllite in low-grade metamorphic rocks rich in aluminous smectites. *Neues Jahrb.  
834 fur Mineral. Monatshefte* 135–144.

835 Kodolányi, J., Pettke, T., Spandler, C., Kamber, B.S., Ling, K.G., 2012. Geochemistry of ocean  
836 floor and fore-arc serpentinites: Constraints on the ultramafic input to subduction zones.  
837 *J. Petrol.* 53, 235–270. <https://doi.org/10.1093/petrology/egr058>

838 Lanson, B., Lantenois, S., van Aken, P.A., Bauer, A., Plancon, A., 2012. Experimental  
839 investigation of smectite interaction with metal iron at 80 C: Structural characterization of

840 newly formed Fe-rich phyllosilicates. *Am. Mineral.* 97, 864–871.  
841 <https://doi.org/10.2138/am.2012.4062>

842 Lantenois, S., Lanson, B., Muller, F., Bauer, A., Jullien, M., Plançon, A., 2005. Experimental  
843 study of smectite interaction with metal Fe at low temperature: 1. Smectite destabilization.  
844 *Clays Clay Miner.* 53, 597–612. <https://doi.org/10.1346/CCMN.2005.0530606>

845 Le Pape, P., Rivard, C., Pelletier, M., Bihannic, I., Gley, R., Mathieu, S., Salsi, L., Migot, S.,  
846 Barres, O., Villiéras, F., Michau, N., 2015. Action of a clay suspension on an Fe(0) surface  
847 under anoxic conditions: Characterization of neoformed minerals at the Fe(0)/solution and  
848 Fe(0)/atmosphere interfaces. *Appl. Geochemistry* 61, 62–71.  
849 <https://doi.org/10.1016/j.apgeochem.2015.05.008>

850 Li, H., Li, Y., Xiang, L., Huang, Q., Qiu, J., Zhang, H., Sivaiah, M.V., Baron, F., Barrault, J.,  
851 Petit, S., Valange, S., 2015. Heterogeneous photo-Fenton decolorization of Orange II over  
852 Al-pillared Fe-smectite: Response surface approach, degradation pathway, and toxicity  
853 evaluation. *J. Hazard. Mater.* 287, 32–41. <https://doi.org/10.1016/j.jhazmat.2015.01.023>

854 McNaught, A.D., Wilkinson, A. (Eds.), 1997. IUPAC. Compendium of Chemical Terminology,  
855 2nd ed. Blackwell Scientific Publications, Oxford.

856 Meunier, A., Petit, S., Cockell, C.S., El Albani, A., Beaufort, D., 2010. The Fe-rich clay  
857 microsystems in basalt-komatiite lavas: Importance of Fe-Smectites for Pre-Biotic  
858 molecule catalysis during the Hadean eon. *Orig. Life Evol. Biosph.* 40, 253–272.  
859 <https://doi.org/10.1007/s11084-010-9205-2>

860 Miyawaki, R., Tomura, S., Samejima, S., Okazaki, M., Misuta, H., Maruyama, S., Shibasaki,  
861 Y., 1991. Effects of Solution Chemistry on the Hydrothermal Synthesis of Kaolinite. *Clays*  
862 *Clay Miner.* 39, 498–508. <https://doi.org/10.1346/CCMN.1991.0390505>

863 Mizutani, T., Fukushima, Y., Okada, A., Kamigaito, O., Kobayashi, T., 1991. Synthesis of 1:1  
864 and 2:1 Iron Phyllosilicates and Characterization of their Iron State by Mössbauer  
865 Spectroscopy. *Clays Clay Miner.* 39, 381–386.  
866 <https://doi.org/10.1346/CCMN.1991.0390407>

867 Mosser-Ruck, R., Cathelineau, M., Guillaume, D., Charpentier, D., Rousset, D., Barres, O.,  
868 Michau, N., 2010. Effects of Temperature, pH, and Iron/Clay and Liquid/Clay Ratios on  
869 Experimental Conversion of Dioctahedral Smectite to Berthierine, Chlorite, Vermiculite,  
870 or Saponite. *Clays Clay Miner.* 58, 280–291.  
871 <https://doi.org/10.1346/CCMN.2010.0580212>

872 Mosser-Ruck, R., Pignatelli, I., Bourdelle, F., Abdelmoula, M., Barres, O., Guillaume, D.,  
873 Charpentier, D., Rousset, D., Cathelineau, M., Michau, N., 2016. Contribution of long-  
874 term hydrothermal experiments for understanding the smectite-to-chlorite conversion in  
875 geological environments. *Contrib. to Mineral. Petrol.* 171, 1–21.  
876 <https://doi.org/10.1007/s00410-016-1307-z>

877 Neumann, A., Sander, M., Hofstetter, T.B., 2011. Redox Properties of Structural Fe in Smectite  
878 *Clay Minerals BT - Aquatic Redox Chemistry. Aquat. Redox Chem.* 1071, 361–379.

879 Noguera, C., Fritz, B., Clément, A., Baronnet, A., 2006a. Nucleation, growth and ageing  
880 scenarios in closed systems I: A unified mathematical framework for precipitation,  
881 condensation and crystallization. *J. Cryst. Growth* 297, 180–186.  
882 <https://doi.org/10.1016/j.jcrysgr.2006.08.049>

883 Noguera, C., Fritz, B., Clément, A., Baronnet, A., 2006b. Nucleation, growth and ageing  
884 scenarios in closed systems II: Dynamics of a new phase formation. *J. Cryst. Growth* 297,  
885 187–198. <https://doi.org/10.1016/j.jcrysgr.2006.08.048>

886 Nriagu, J.O., 1975. Thermochemical approximations for clay minerals. *Am. Mineral.* 60, 834–  
887 839.

888 Osacký, M., Šucha, V., Czímerová, A., Pentrák, M., Madejová, J., 2013. Reaction of smectites  
889 with iron in aerobic conditions at 75°C. *Appl. Clay Sci.* 72, 26–36.  
890 <https://doi.org/10.1016/j.clay.2012.12.010>

891 Parkhurst, D.L., Appelo, C.A.J., 2013. Description of input and examples for PHREEQC  
892 version 3 - A computer program for speciation, batch-reaction, one-dimensional transport  
893 and inverse geochemical calculations.

894 Pedreira-Segade, U., Feuillie, C., Pelletier, M., Michot, L.J., Daniel, I., 2016. Adsorption of  
895 nucleotides onto ferromagnesian phyllosilicates: Significance for the origin of life.  
896 *Geochim. Cosmochim. Acta* 176, 81–95. <https://doi.org/10.1016/j.gca.2015.12.025>

897 Peretyazhko, T.S., Sutter, B., Morris, R. V., Agresti, D.G., Le, L., Ming, D.W., 2016. Fe/Mg  
898 smectite formation under acidic conditions on early Mars. *Geochim. Cosmochim. Acta*  
899 173, 37–49. <https://doi.org/10.1016/j.gca.2015.10.012>

900 Petit, S., Baron, F., Decarreau, A., 2017. Synthesis of nontronite and other Fe-rich smectites : a  
901 critical review. *Clay Miner.* 52, 469–483. <https://doi.org/10.1180/claymin.2017.052.4.05>

902 Pignatelli, I., Bourdelle, F., Bartier, D., Mosser-Ruck, R., Truche, L., Mugnaioli, E., Michau,  
903 N., 2014. Iron-clay interactions: Detailed study of the mineralogical transformation of  
904 claystone with emphasis on the formation of iron-rich T-O phyllosilicates in a step-by-step  
905 cooling experiment from 90°C to 40°C. *Chem. Geol.* 387, 1–11.  
906 <https://doi.org/10.1016/j.chemgeo.2014.08.010>

907 Pignatelli, I., Mugnaioli, E., Hybler, J., Mosser-Ruck, R., Cathelineau, M., Michau, N., 2013.  
908 A multi-technique characterization of cronstedtite synthesized by iron-clay interaction in

909 a step-by-step cooling procedure. *Clays Clay Miner.* 61, 277–289.  
910 <https://doi.org/10.1346/CCMN.2013.0610408>

911 Pokrovski, G.S., Schott, J., Farges, F., Hazemann, J.L., 2003. Iron (III)-silica interactions in  
912 aqueous solution: Insights from X-ray absorption fine structure spectroscopy. *Geochim.*  
913 *Cosmochim. Acta* 67, 3559–3573. [https://doi.org/10.1016/S0016-7037\(03\)00160-1](https://doi.org/10.1016/S0016-7037(03)00160-1)

914 Pokrovski, G.S., Schott, J., Hazemann, J., Farges, F., Pokrovsky, Oleg, S., 2002. An X-ray  
915 absorption fine structure and nuclear magnetic resonance spectroscopy study of gallium–  
916 silica complexes in aqueous solution. *Geochim. Cosmochim. Acta* 66, 4203–4322.

917 Reynolds, R.C., DiStefano, M.P., Lahann, R.W., 1992. Randomly interstratified  
918 serpentine/chlorite; its detection and quantification by powder X-ray diffraction methods.  
919 *Clays Clay Miner.* 40, 262 LP-267.

920 Rivard, C., Montargès-Pelletier, E., Vantelon, D., Pelletier, M., Karunakaran, C., Michot, L.J.,  
921 Villieras, F., Michau, N., 2013. Combination of multi-scale and multi-edge X-ray  
922 spectroscopy for investigating the products obtained from the interaction between  
923 kaolinite and metallic iron in anoxic conditions at 90 °C. *Phys. Chem. Miner.* 40, 115–  
924 132. <https://doi.org/10.1007/s00269-012-0552-6>

925 Rivard, C., Pelletier, M., Michau, N., Razafitianamaharavo, A., Abdelmoula, M., Ghanbaja, J.,  
926 Villiéras, F., 2015. Reactivity of callovo-oxfordian claystone and its clay fraction with  
927 metallic Iron: Role of non-clay minerals in the interaction mechanism. *Clays Clay Miner.*  
928 63, 290–310. <https://doi.org/10.1346/CCMN.2015.0630404>

929 Roy, D.M., Roy, R., 1954. An experimental study of the formation and properties of synthetic  
930 serpentines and related layer silicate minerals. *Am. Mineral.* 53, 957–975.

931 Snow, C.L., Lee, C.R., Shi, Q., Boerio-Goates, J., Woodfield, B.F., 2010a. Size-dependence of

932 the heat capacity and thermodynamic properties of hematite ( $\alpha$ -Fe<sub>2</sub>O<sub>3</sub>). *J. Chem.*  
933 *Thermodyn.* 42, 1142–1151. <https://doi.org/10.1016/j.jct.2010.04.009>

934 Snow, C.L., Shi, Q., Boerio-Goates, J., Woodfield, B.F., 2010b. Heat Capacity Studies of  
935 Nanocrystalline Magnetite (Fe<sub>3</sub>O<sub>4</sub>). *J. Phys. Chem. C* 114, 21100–21108.  
936 <https://doi.org/10.1021/jp1072704>

937 Snow, C.L., Smith, S.J., Lang, B.E., Shi, Q., Boerio-Goates, J., Woodfield, B.F., Navrotsky,  
938 A., 2011. Heat capacity studies of the iron oxyhydroxides akaganéite ( $\beta$ -FeOOH) and  
939 lepidocrocite ( $\gamma$ -FeOOH). *J. Chem. Thermodyn.* 43, 190–199.  
940 <https://doi.org/10.1016/j.jct.2010.08.022>

941 Sposito, G., 1986. The polymer model of thermochemical clay mineral stability. *Clays Clay*  
942 *Miner.* 34, 198–203. <https://doi.org/10.1346/CCMN.1986.0340210>

943 Sreedhar, B., Arundhathi, R., Reddy, M.A., Parthasarathy, G., 2009. Highly efficient  
944 heterogenous catalyst for acylation of alcohols and amines using natural ferrous  
945 chamosite. *Appl. Clay Sci.* 43, 425–434. <https://doi.org/10.1016/j.clay.2008.10.001>

946 Stølen, S., Glöckner, R., Grønvold, F., Atake, T., Izumisawa, S., 1996. Heat capacity and  
947 thermodynamic properties of nearly stoichiometric wüstite from 13 to 450 K. *Am.*  
948 *Mineral.* 81, 973–981. <https://doi.org/10.2138/am-1996-7-819>

949 Stucki, J.W., 2013. Properties and Behaviour of Iron in Clay Minerals, in: Bergaya, F., Lagaly,  
950 G. (Eds.), *Handbook of Clay Science Fundamentals*. Elsevier, pp. 559–611.  
951 <https://doi.org/10.1016/B978-0-08-098258-8.00018-3>

952 Stucki, J.W., Goodman, B.A., Schwertmann, U. (Eds.), 1989. *Iron in Soils and Clay Minerals*,  
953 *Soil Science*. D. Reidel Publishing Company. [https://doi.org/10.1097/00010694-](https://doi.org/10.1097/00010694-198904000-00013)  
954 [198904000-00013](https://doi.org/10.1097/00010694-198904000-00013)

955 Tardy, Y., Fritz, B., 1981. An ideal solid solution model for calculating solubility of clay  
956 minerals. *Clay Miner.* 361–373.

957 Tardy, Y., Garrels, R.M., 1974. A method of estimating the Gibbs energies of formation of  
958 layer silicates. *Geochim. Cosmochim. Acta* 38, 1101–1116. <https://doi.org/10.1016/0144->  
959 [2449\(86\)90007-2](https://doi.org/10.1016/0144-2449(86)90007-2)

960 Tosca, N.J., Guggenheim, S., Pufahl, P.K., 2016. An authigenic origin for Precambrian  
961 greenalite: Implications for iron formation and the chemistry of ancient seawater. *Geol.*  
962 *Soc. Am. Bull.* 128, 511–530. <https://doi.org/10.1130/B31339.1>

963 Trujillano, R., Rico, E., Vicente, M.A., Rives, V., Chaabene, B.E.N., Ghorbel, A., 2009.  
964 Microwave-Assisted Synthesis of Fe<sup>3+</sup> Saponites. Characterization by X-Ray Diffraction  
965 and FT-IR Spectroscopy. *Rev. la Soc. española Mineral.* 11, 189–190.

966 Van Hise, C.R., Leith, C.K., 1911. Precipitation of greenalite, in: *The Geology of Lake Superior*  
967 *Region.* U.S. Geological Survey, Washington, 521–525.

968 Vieillard, P., 2000. A new method for the prediction of Gibbs free energies of formation of  
969 hydrated clay minerals based on the electronegativity scale. *Clays Clay Miner.* 48, 459–  
970 473. <https://doi.org/10.1346/CCMN.2000.0480406>

971 Vieillard, P., 1994. Prediction of enthalpy of formation based on refined crystal structures of  
972 multisite compounds: Part 1. Theories and examples. *Geochim. Cosmochim. Acta* 58,  
973 4049–4063. [https://doi.org/10.1016/0016-7037\(94\)90266-6](https://doi.org/10.1016/0016-7037(94)90266-6)

974 Wang, X., Dong, H., Zeng, Q., Xia, Q., Zhang, L., Zhou, Z., 2017. Reduced Iron-Containing  
975 Clay Minerals as Antibacterial Agents. *Environ. Sci. Technol.* 51, 7639–7647.  
976 <https://doi.org/10.1021/acs.est.7b00726>



- 977 Wilkins, R.W.T., Ito, J., 1967. Infrared Spectra of Some Synthetic Talcs. *Am. Mineral.* 52,  
978 1649–1661.
- 979 Wilson, J.C., Benbow, S., Sasamoto, H., Savage, D., Watson, C., 2015. Thermodynamic and  
980 fully-coupled reactive transport models of a steel–bentonite interface. *Appl. Geochemistry*  
981 61, 10–28. <https://doi.org/10.1016/j.apgeochem.2015.05.005>
- 982 Zhang, D., Zhou, C.-H., Lin, C.-X., Tong, D.-S., Yu, W.-H., 2010. Synthesis of clay minerals.  
983 *Appl. Clay Sci.* 50, 1–11. <https://doi.org/10.1016/j.clay.2010.06.019>
- 984 Zolotov, M.Y., 2015. Formation of brucite and cronstedtite-bearing mineral assemblages on  
985 Ceres. *Icarus* 228, 13–26. <https://doi.org/10.1016/j.icarus.2013.09.020>